Journal of Inflammation Research

Dovepress
open access to scientific and medical research

Open Access Full Text Article

ORIGINAL RESEARCH

Qing-Luo-Yin Eased Adjuvant-Induced Arthritis by Inhibiting SIRT1-Controlled Visfatin Production in White Adipose Tissues

Dan-Dan Wang[1,2,*], Meng-Ke Song[1,3,*], Qin Yin[1,2], Wen-Gang Chen[2], Opeyemi Joshua Olatunji[4], Kui Yang[3], Jian Zuo[1,3,5]

[1]Xin'an Medicine Research Center, The First Affiliated Hospital of Wannan Medical College (Yijishan Hospital), Wuhu, 241000, People's Republic of China; [2]Department of Pharmacy, the Second Affiliated Hospital of Wannan Medical College, Wuhu, 241000, People's Republic of China; [3]Research Center of Integration of Traditional Chinese and Western Medicine, Wannan Medical College, Wuhu, 241000, People's Republic of China; [4]African Genome Center, Mohammed VI Polytechnic University, Ben Guerir, 43150, Morocco; [5]Anhui Province Key Laboratory of Non-Coding RNA Basic and Clinical Transformation, Wannan Medical College, Wuhu, 241000, People's Republic of China

*These authors contributed equally to this work

Correspondence: Kui Yang; Jian Zuo, Email ykui15556689670@163.com; zuojian8178@163.com

Background: Nicotinamide adenine dinucleotide (NAD)-dependent deacetylase SIRT1 regulates both metabolism and immune functions. This study investigated if SIRT1 inhibitory property of herbal formula Qing-Luo-Yin (QLY) contributed to its anti-rheumatic effects.

Methods: Adjuvant-induced arthritis (AIA) rats were treated by QLY and nicotinamide mononucleotide (NMN, a biosynthesis precursor of NAD) for 38 days. After sacrifice, blood, paws, liver and white adipose tissues (WAT) were collected. Pre-adipocytes were cultured by the rats' serum. The medium was used for monocytes culture. Some pre-adipocytes were treated by QLY-derived SIRT1 inhibitors. *SIRT1* was silenced or overexpressed beforehand. The samples were subjected to kits-based quantification, polymerase-chain reaction, western-blot, immunofluorescence, and histology experiments.

Results: AIA rats experienced significant fat loss in liver and WAT. Expression of many SIRT1-related signals like PPARγ, PGC-1α, HSL, ATGL and CPT-1A were altered. QLY attenuated all these abnormalities and joint injuries. By pan-acetylation up-regulation, visfatin was obviously reduced in QLY-treated AIA rats' blood (from 191.8 to 127.0 pg/mL). NMN sustained SIRT1 activation by replenishing NAD, and weakened these effects. QLY-containing serum and the related compounds showed similar impacts on pre-adipocytes, resembling the changes in QLY-treated AIA rats' WAT. These treatments suppressed AIA serum-induced visfatin secretion (from 49.3 to 36.1 and 30.7 pg/mL). This effect was impaired by *SIRT1* overexpression. The medium from the compounds-treated pre-adipocytes impaired NF-κB activation in AIA serum-cultured monocytes.

Conclusion: Besides fat depletion, SIRT1 up-regulation in rheumatic subjects' WAT promotes visfatin production, and exacerbates inflammation. SIRT1 inhibition in WAT is an anti-rheumatic way of QLY independent of immune regulation.

Keywords: visfatin, PPARγ, rheumatoid arthritis, Traditional Chinese Medicine, adipocyte

Introduction

Rheumatoid arthritis (RA) is characterized by an initial state of autoimmune reactions, which eventually leads to persistent inflammation and tissue degradation in joints.[1] RA progression is predominantly driven by T cells. Their hyper-activation culminates in disruption of cytokines network. Increase of inflammatory cytokines like IL-1, IL-6, and IL-17 directly accounts for most of RA-related manifestations.[2] It should be aware that monocytes/macrophages are key sources of these factors too, which contribute to RA pathology in multiple aspects. They activate T lymphocytes and many effector cells, differentiate toward osteoblasts, and drive synovial angiogenesis.[3–6] In brief, macrophages and the precursors (monocytes) show inflammatory phenotype in RA.[5–7] Their functional shift is an indicator of RA

Received: 19 June 2024
Accepted: 17 September 2024
Published: 24 September 2024

progression.[8] Any approaches that can affect their polarization would possibly benefit RA patients. Conventional anti-RA therapies typically include non-steroidal anti-inflammatory drugs, glucocorticoids and disease-modifying antirheumatic drugs. Many of them exhibit potentials in regulating monocytes/macrophages.[4,9] Benefited from the significant advance in RA pathology, novel biological agents are applied in treating RA, represented by TNF-α neutralizing antibodies and selective JAK inhibitors, which are designed to preferentially abrogate pathological differentiation and functions of lymphocytes.[10] More endeavors should be devoted to develop monocytes/macrophages-targeting drugs.

Beyond immune mediators, energy metabolism status represents another critical determinant for functions of monocytes/macrophages.[11] When activated, they rely on glycolytic pathway.[12] Indispensable metabolites from Kreb's cycle are replenished by glutamine metabolism then.[13] At the same time, their triglyceride-utilizing ability is impaired. This change reinforces phagocytosis by providing more lipids to construct plasma membranes.[14] All the above abnormalities are witnessed in RA patients. As the result, metabolic intervention becomes a plausible therapeutic strategy.[15] The signals simultaneously controlling metabolism and immune functions therefore draw intense attentions. Nicotinamide adenine dinucleotide (NAD)-dependent deacetylase SIRT1 is a good representative. It regulates PPARγ and PGC-1α to promote fat catabolism and oxidative phosphorylation, and inhibits transcriptional activities of AP-1, HIF-1α and NF-κB via deacetylation.[16] It is widely believed that SIRT1 activation will hamper inflammatory polarization of monocytes/macrophages and is beneficial in controlling RA.[17] But we should be aware that SIRT1 is generally overexpressed in RA patients' synovial cells, where it induces inflammatory secretion and apoptosis resistance.[18] We had similarly observed SIRT1 up-regulation in rheumatic subjects, especially during inflammatory stages.[8,19] Possibly, in certain tissues SIRT1 plays a pro-inflammatory role. A proof is that SIRT1 controls production of visfatin, which is the secreted form of NAMPT (a rate-limiting enzyme of NAD biosynthesis).[20] As an adipokine, visfatin is predominantly secreted by white adipose tissues (WAT). Acting as a TLR4 agonist, it potently activates monocytes/macrophages. Besides, visfatin facilitates glycolysis by sustaining NAD supply.[21] Because its increase in RA is obvious, visfatin has been recognized as an anti-rheumatic target.[22]

Qing-Luo-Yin (QLY) is a herbal formula prescribed by a Traditional Chinese Medicine (TCM) master Ji-Ren Li, and demonstrates impressive effects in treating RA.[23] We found that QLY inhibited inflammatory differentiation of immune cells and restored metabolic balance in rheumatic subjects.[23–25] A recent work has shown that the outcomes are possibly related to SIRT1 inhibition, as many related compounds are potential SIRT1 inhibitors, including berberine, matrine, sophocarpine, sinomenine, palmatine and dioscin, and QLY therapy reduced visfatin secretion efficiently.[26] But if SIRT1 inhibition indeed contributes to its anti-rheumatic effects in vivo was yet to be confirmed. This study aimed to answer this question using adjuvant-induced arthritis (AIA) rats. Some rats were given with nicotinamide mononucleotide (NMN, a direct biosynthesis precursor of NAD) to provoke SIRT1 activation. It does not only further clarify the anti-rheumatic mechanism of QLY but also confirms that SIRT1/visfatin inhibition in WAT is an approach to suppress inflammatory polarization of residential monocytes/macrophages. Besides, it challenges the belief that SIRT1 up-regulation is always favorable for anti-inflammatory treatments, inspiring us to re-think the rational application of SIRT1 agonists.

Material and Methods

Reagents

Heat-inactivated Bacillus Calmette-Guérin (BCG) and incomplete Freund's adjuvant (IFA) were supplied by Rebio Scientific (Shanghai, China). ELISA quantification kits of IL-1β, IL-6, IL-17A, MCP-1, TNF-α, leptin, and adiponectin were purchased from MultiScience Biotech (Hangzhou, Zhejiang, China). Colorimetric quantification kits of reduced glutathione (GSH), malonaldehyde (MDA), superoxide dismutase (SOD), alkaline phosphatase (AKP), glycated serum protein (GSP), glucose (GLU), lactic acid (LA), triglyceride (TG), total cholesterol (T-CHO), high-density lipoprotein cholesterol (HDL-C), and low-density lipoprotein cholesterol (LDL-C) together with visfatin ELSIA kit were supplied by Jiancheng Bioengineering Institute (Nanjing, Jiangsu, China). Primary antibodies and HRP/fluorescein-conjugated secondary antibodies were provided by Affinity Biosciences (Changzhou, Jiangsu, China) and Boster Biological Technology (Wuhan, China), respectively. SIRT1 overexpression plasmid was constructed by General Biol (Chuzhou,

Anhui, China) based on pcDNA3.1-EGFP vector. Primers and siRNA were synthesized by Universal Biology (Chuzhou, Anhui, China), and their sequences are shown in Table S1. NMN, bovine serum albumin (BSA) and fetal bovine serum (FBS) were procured from Sigma-Aldrich (St Louis, MO, USA). Matrine, sinomenine, sophocarpine, dioscin, and berberine were the products of Bencao Yikang Biotechnology (Nanjing, Jiangsu, China). All the other reagents used were obtained from domestic suppliers.

Preparation of QLY Extract

Raw herbal drugs including Kushen (radix of *Sophora flavescens* Ait)., Qingfengteng [caulis of *Sinomenium acutum* (Thunb). Rehder and E. H. Wilson], Huangbai (cortex of *Phellodendron chinense* C. K. Schneid)., and Bixie [rhizome of *Dioscorea collettii var. hypoglauca* (Palib). S. J. Pei and C. T. Ting] were brought from Bozhou Herbal Medicine Market (Anhui, China), and authenticated by Professor Jian Zuo (Wannan Medical College, Anhui, China). The voucher specimens were kept in the Herbarium Center of Wannan Medical College (ID: 2022–013). These ingredients were combined in a ratio of 1.5: 1.2: 1: 1, and pulverized. The powder underwent reflux extraction with 95% ethanol twice. The residues were further boiled in water for one time. The combined filtrates were dried to yield a sticky extract. For the administration use, this product was dissolved in ethanol, and evenly dispersed in 0.5% CMC-Na solution. Ethanol content in the suspension is about 1.2%.

Establishment of AIA Model in Rats and Treatments

The animal experiment procedures were strictly adhered to ARRIVE guidelines, and received the approval from the Ethics Committee of Wannan Medical College (Ethics Approval Number: WNMC-AWE-2023358). A group of 32 male SD rats (7-weeks old, obtained from Tianqin Biotechnology) were housed in a specific-pathogens free laboratory, and acclimated for 1 week before any experimental procedures. BCG was first grinded in a mortar carefully, and mixed with IFA to prepare complete Freund's adjuvant (CFA, containing 10 mg/mL of BCG). The rats were randomly assigned into four groups, three of which received an intradermal injection of CFA (0.1 mL) at the plantar skin of left hind paw.

The untreated rats served as the normal control group (normal). The immunized rats were administered with 0.5% CMC-Na, QLY or QLY in the combination of NMN by gavage, and they were recorded as AIA, QLY and QLY+NMN groups, respectively. We had investigated the dose-dependent therapeutic effects of QLY on a RA model.[26] To minimize the use of rats, only one optimal dose (0.45 g/kg/day of raw drugs) was adopted here based on body surface area-based equivalent dose calculation. Because anti-rheumatic effects of QLY had been thoroughly investigated, no control drug was included in the current study, which focused on the therapeutic mechanism.[23–26] The treatment dose of NMN was set at 200 mg/kg/day.[27]

Therapeutic Effects Evaluation

Ten days after CFA immunization, AIA progression was periodically evaluated based on arthritis scores by two scholars who were blinded to the experiment arrangement. The quantification criterion was reported previously.[26] The rats failing to develop secondary inflammation were excluded in the following experiments. Finally, 6 rats in each group were kept. After the treatments for 38 days, all the rats were anesthetized by an intraperitoneal injection of pentobarbital sodium (30 mg/kg), and a maximum amount of blood was collected through abdominal aorta until death. Hind paws, liver, and perirenal fat pads were immediately removed and weighed.

After centrifugation, blood plasma and serum were obtained, which were used in quantification tests and cell culture. Monocytes were isolated from fresh anticoagulant blood using a separation kit (Solarbio Biotech, Beijing, China). Expression levels of the genes involved in monocyte polarization were evaluated by quantitative reverse transcription polymerase-chain reaction (qRT-PCR) assays.

Parts of tissue samples were fixed, embedded in paraffin, and sectioned. Liver sections were subjected to Oil Red O staining-based histological examination. Other tissues were dyed with hematoxylin-eosin (H&E). The experiments followed the same steps as previously described.[28,29] The stained sections were observed by an Olympus BH-2 optical microscope (Tokyo, Japan). Some sections of rat WAT were used in immunofluorescence (IF) assays to observe expression of visfatin and pan-acetylated proteins with the procedures below. The remaining tissue samples were homogenized. A portion of

the homogenates were subjected to quantification tests, and expression of SIRT1, (ace)-PPARγ, PGC-1α, HSL ATGL, CPT-1A and IL-1β was investigated by western-blot (WB) method using the other portion of these homogenates. In addition, ace-PPARγ expression in WAT was detected by immunoprecipitation (IP) method.

Cells Isolation and Culture

Primary monocytes were isolated from healthy rats' blood using the aforementioned kit according to the manufacturer's instruction. To prepare pre-adipocytes, WAT from healthy rats was digested using collagenase I. After centrifugation, the precipitated cells were immediately cultured in DMEM/F12 medium supplemented with 10% FBS and penicillin-streptomycin (100 U/mL). Rat monocytes were used for once without further passage, while homogeneous fibroblast-like pre-adipocytes from the 3rd to 8th passages were used. Some experiments used human THP-1 monocytes and mouse 3T3-L1 pre-adipocytes. The two cell lines were brought from Pricella Biotechnology (Wuhan, Hubei, China), which were originally from ATCC and passed STR tests. All the cells were grown in complete DMEM/F12 medium at 37°C in a humidified atmosphere with 5% CO_2. They were passaged in a ratio of 1: 3 when reaching 80% of confluence.

Treatments of Cells In vitro

Rat pre-adipocytes were seeded in a 24-well plate (2×10^5 cells/well), and cultured in normal FBS-containing medium. After cells adhered to wall, supernatants in the wells were replaced by the mediums prepared using 10% different serums from the in vivo experiments. Twenty-four hours later, the cells were collected for WB assays, while levels of certain metabolites and cytokines in the medium were determined by the corresponding kits. This cell culture was repeated, and the medium supernatants were collected for further use. Monocytes were seeded in a 24-well plate (3×10^5 cells/well), and cultured for 12 h beforehand. Subsequently, half of supernatants in the wells were replaced by the aforementioned mediums. Another 24 h culture was conducted, and the medium was finally collected for ELSIA analysis. In a replicate experiment, rat monocytes were cultured by the medium containing 10% supernatants of rats' WAT homogenates after attachment.

Some other rat pre-adipocytes seeded in 6-wells plates (1×10^6 cells/well) were allocated into 4 groups. The cells in one group were cultured in the medium prepared by healthy rats' serum, and the others were cultured in AIA serum-containing medium for 12 h. Then, half of these mediums were replaced by fresh ones. The cells in QLY group were cultured with QLY-treated AIA rats' serum this time, while mediums for the other groups were the same as before. Those continuously grown in healthy and AIA rats' serums were taken as control and AIA groups, respectively. Some AIA rats' serum-cultured cells were treated by QLY-related compounds, including matrine (100 ng/mL), sinomenine (80 ng/mL), sophocarpine (100 ng/mL), dioscin (25 μg/mL), and berberine (25 μg/mL). This round of culture lasted for 24 h. Finally, the cells were collected for WB assays, and the mediums were collected for biochemical or ELISA analyses. Afterwards, we repeated the experiment by using 3T3-L1 cells. Intracellular expression of visfatin and pan-acetylated proteins was observed in an IF experiment. Visfatin levels in the mediums were detected by ELISA method.

To clarify the role of SIRT1 in QLY-caused changes of pre-adipocytes, this gene was silenced or overexpressed in the following experiments. Rat pre-adipocytes were seeded in 6-well plates (1×10^6 cells/well). When reaching 40% of confluence, some cells were treated by siRNA-SIRT1 (100 nM) along with Lipofectamine 2000 reagent (Invitrogen, Shanghai, China). In another experiment, SIRT1 overexpression plasmid (100 nM) was transfected into the cells using Lipofectamine 3000 reagent (Invitrogen, Shanghai, China). The other arrangements, including rat serum culture and chemical stimulus were the same as above. The pre-adipocytes were subjected to WB assays, and a portion of the mediums were used to detect cytokines and metabolites. Next, we cultured THP-1 monocytes in 6-well plates at a density of 2×10^6 cells/well. After cell attachment, supernatants in the wells were replaced by some mediums from the above pre-adipocytes culture assay. After being cultured for 4 h, intracellular expression and localization of visfatin and p65 subunit were investigated by IF method.

qRT-PCR, WB and IP Assays

Trizol reagent (Tiangen, Beijing, China) was used to extract total RNA from cells, and the product was reverse-transcribed into cDNA by the aid of a synthesis kit. qRT-PCR experiments were conducted using Universal qPCR Master Mix kits on a 7500 Real-Time PCR Detection System (Applied Biosystems, Life Technologies). cDNA served as the templates. Relative mRNA expression was calculated by the $2^{\wedge(-\Delta\Delta CT)}$ method with *β-ACTIN* as the internal reference gene.[30,31]

Tissue or cell samples were added into the RIPA buffer containing PMSF and a protease inhibitor mixture (Beyotime, Shanghai, China). The mixture was then lysed on ice for 30 min to 2 h and centrifuged. Protein contents in the supernatants were determined by a quantification kit (Beyotime, Shanghai, China). The protein samples underwent electrophoresis on SDS polyacrylamide gels, and the separated proteins were transferred onto nitrocellulose membranes in ice-water. After being blocked with 5% BSA, the membranes were incubated overnight at 4°C with primary antibodies. Afterwards, they were washed three times, followed by incubation with appropriate HRP-conjugated secondary antibodies at room temperature for 1 h.[32] Protein signals were visualized using a detection reagent on an Amersham Imager 600 ECL Imaging System. Relative expression levels of protein were normalized to β-ACTIN/GAPDH by the aid of Image J software (1.52a, NIH, Bethesda, MD, USA).

In IP assay, WAT RIPA lysates were incubated with protein A/G magnetic beads in the diluted primary pan-acetylation (ace-lys) antibody solution at 4°C overnight. Proteins bound to the beads were extracted by boiling loading buffer. PPARγ concentrations in this product were assessed by WB method.[33,34]

IF Experiment

Tissue sections and cells were first treated by 0.1% Triton solution for 10 min. After extensive washing, 5% BSA-based blocking procedure was performed. Primary rabbit anti-rat/human NAMPT/visfatin and mouse anti-rat/human pan ace-lys/p65 antibodies (1: 100) were added, and an overnight incubation at 4°C was carried out. The samples were then treated with fluorescein-labeled secondary IgG antibodies (1: 500) at room temperature for 1 h. Finally, cell nucleus was stained by DAPI. After being sealed with an anti-fade mounting reagent, the processed samples were observed by a Leica SP8 Lightning confocal microscope.

Statistical Analysis

Each group in vivo and in vitro experiments included 6 and 5 replicates, respectively. All WB experiments were performed in triplicates. Data were presented in the form of mean and standard deviation (SD). Shapiro–Wilk test and Bartlett's test were adopted to check normality and homogeneity of variance, respectively. Statistical differences among groups were evaluated by one-way analysis of variance (ANOVA) followed by Tukey's post hoc test with the aid of GraphPad Prism 8.0 (GraphPad Software, Cary, NC, USA).

Results

SIRT1 Inhibition Was Involved in the Therapeutic Actions of QLY on AIA Rats

Because cells cannot efficiently utilize extracellular NAD, we used NMN here to fuel the functions of SIRT1. As anticipated, NMN greatly increased both NAD and NADH in HepG2 cells, and suppressed expression of pan-acetylated proteins. QLY-restored ace-PPARγ expression decline in AIA serum-cultured cells was antagonized by NMN (Figure S1). These evidences confirm that NMN supplement is an effective way to sustain SIRT1 activation.

Since day 15, secondary inflammatory became evident in AIA rats. QLY therapy showed notable effects in repressing arthritis scores. But no difference about arthritic severity was observed between AIA and QLY+NMN groups (Figure 1A). This result was supported by weights-based paw edema assessment (Figure 1B). By the end of observation, there was no obvious change about expression of *IL-1β, iNOS, IL-10, Arg-1, MCP-1, SIRT1* and *PPARγ* in the monocytes of AIA rats compared with normal controls. Interestingly, *IL-6* expression was even decreased. It suggests that AIA is a self-limiting condition, and immune hyper-activation would be recovered during later stages. Under this circumstance, neither QLY nor QLY+NMN treatments affected the genes' expression (Figure 1C). The similar results were observed concerning levels of interleukins in plasma, and concentrations of IL-1β, IL-6, and IL-17A in all the rats were similar (Figure 1D). Consequently, oxidative stress markers GSH, MDA, and SOD showed no differences among these groups (Figure 1E). This condition allowed us to focus on involvement of other tissues in AIA. Interestingly, MCP-1 increase was obvious in AIA rats' blood. Because immune status had been rebalanced, WAT could play a pro-inflammatory role then, which is another main source of MCP-1.[35] QLY brought its levels down, while NMN showed no impact on the result, suggesting weak effects of SIRT1 on MCP-1 production in WAT (Figure 1D). Level variation of a bone remodeling indicator AKP was similar to that of paw edema (Figure 1F). Even though inflammation had been spontaneously eased, levels of TNF-α and rheumatoid factor (RF) in

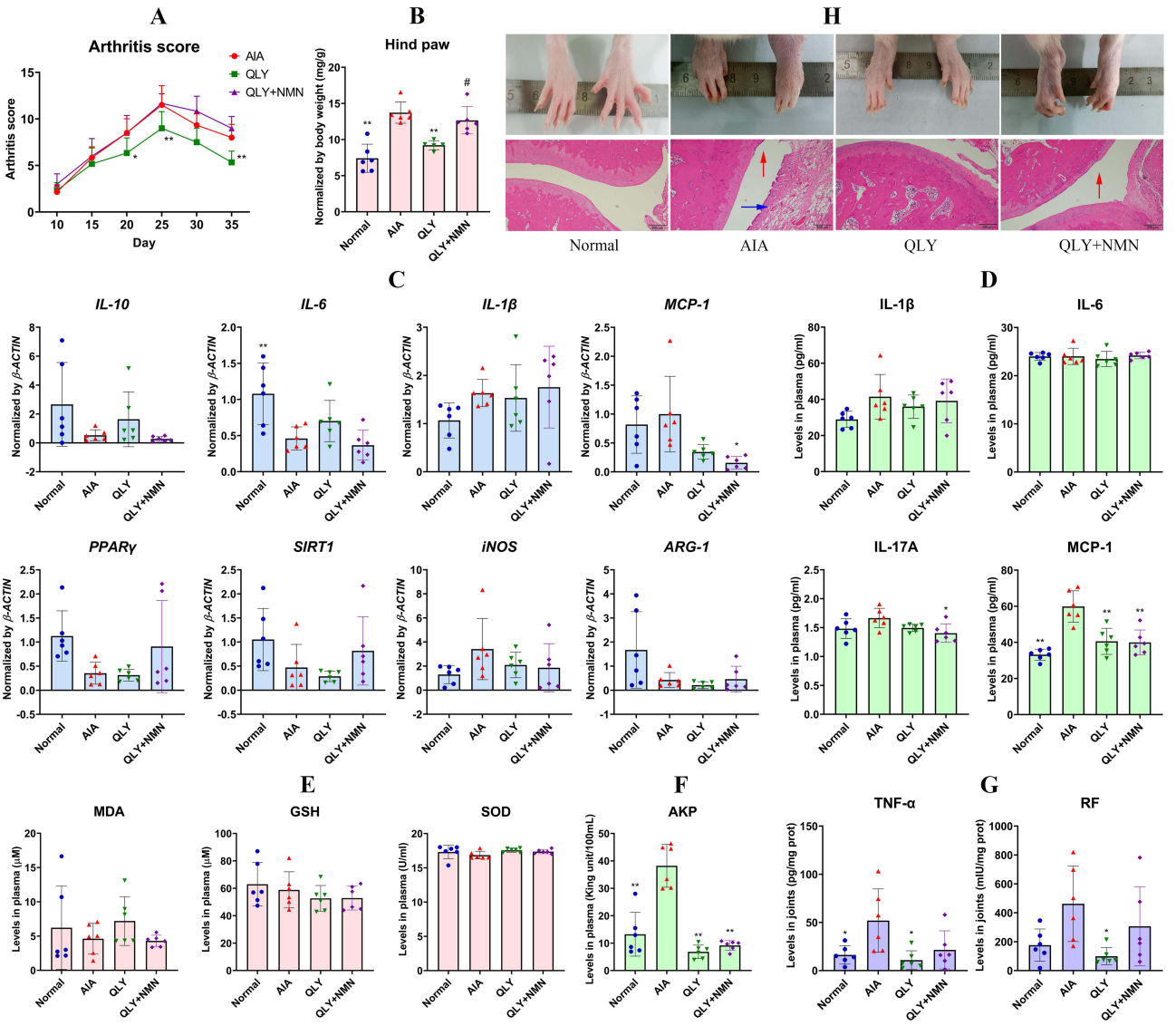

Figure 1 QLY therapy improved arthritic manifestations of AIA rats. (**A**) AIA progression evaluated based on arthritis scores; (**B**) relative weight of left hind paw; (**C**) expression of some polarization-related genes in blood monocytes; (**D**) levels of some RA-related cytokines (IL-1β, IL-6, IL-17A and MCP-1) in rats' blood; (**E**) levels of oxidative indicators (GSH, MDA and SOD) in rats' blood; (**F**) AKP levels in rats' blood; (**G**) levels of TNF-α and RF detected in rats' joints; (**H**) morphological observation and H&E staining-based histological examination of left hind ankle joint; the red and blue arrows indicate cartilage erosion and synovial invasion, respectively. All the data are presented in mean±SD. Statistical significance: *$p < 0.05$ and **$p < 0.01$ compared with AIA models; $^{\#}p < 0.05$ compared with QLY-treated AIA rats.

joints among these groups were still differed. Their increase in AIA rats was suppressed by QLY, while NMN impaired this effect (Figure 1G). Consistent to this finding, AIA rats suffered from visible cartilage erosion and synovial hyperplasia. QLY alleviated all these abnormalities. But cartilage degradation can be still observed in the AIA rats receiving the combination treatment. These histological differences eventually reflected in the varied morphology of paws (Figure 1H).

QLY Inhibited SIRT1 in AIA Rats' Liver

SIRT1 is an important metabolic regulator. To confirm the effects of QLY on SIRT1, we detected some metabolites. Levels of GSP, GLU and LA in AIA rats' blood were altered obviously, showing glycolysis acceleration. Despite TG remained unaffected, levels of T-CHO, HDL-C, and LDL-C were all declined. QLY generally restored all the metabolic changes, and this effect was weakened by NMN (Figure 2A).

The above changes are largely determined by liver, the crucial metabolism hub. Therefore, we investigated changes there. TG and GLU were reduced significantly in AIA rats' liver. The situation was improved by QLY, but this beneficial

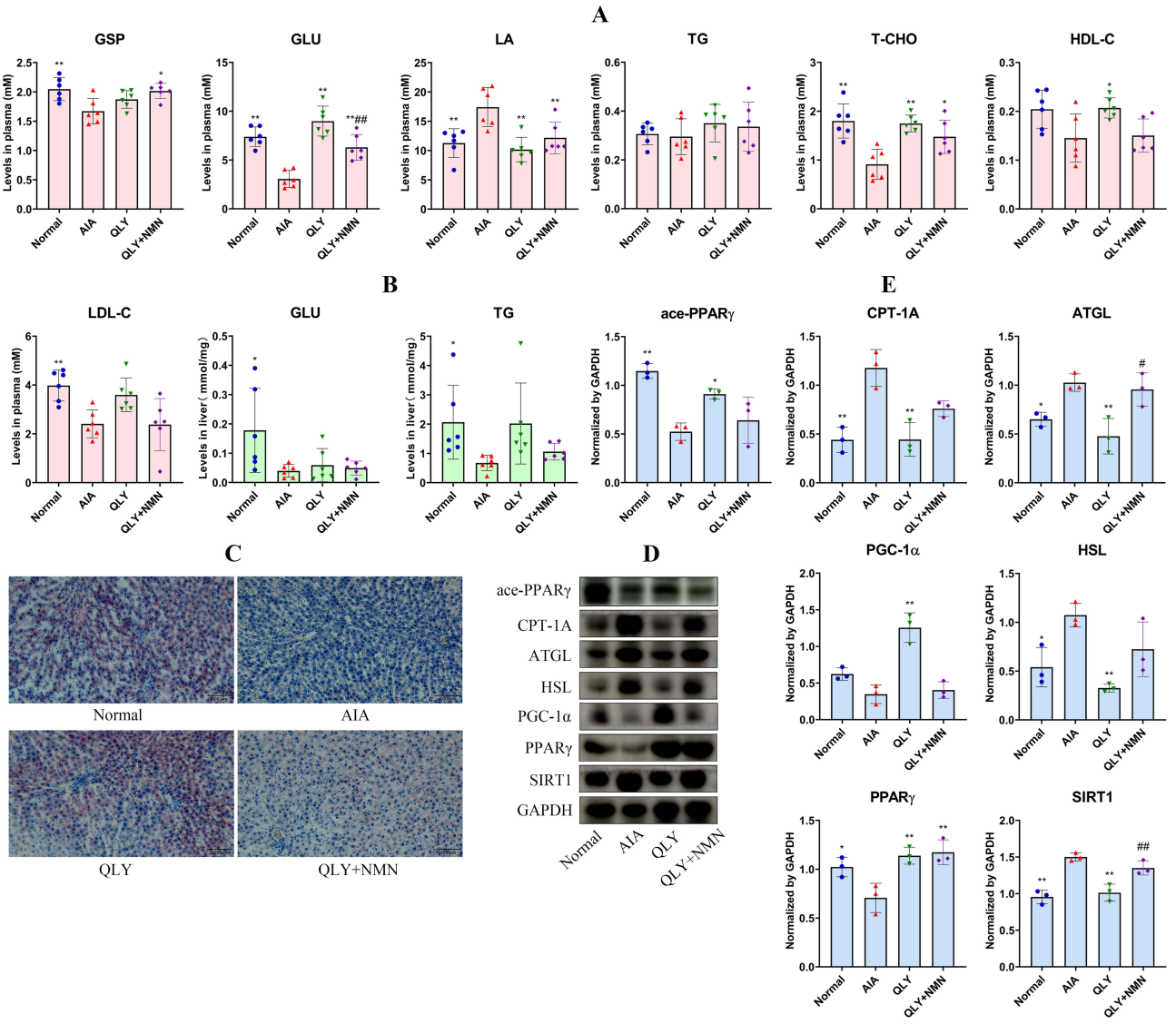

Figure 2 QLY therapy affected SIRT1-related signals as well as metabolic status in AIA rats' liver. (**A**) levels of metabolism indicators in rats' blood; (**B**) levels of GLU and TG in rats' livers; (**C**) Oil Red O staining-based histological examination of livers; (**D**) WB assay performed using liver samples; (**E**) the quantification results of assay (**D**). All the data are presented in mean±SD. Statistical significance: *p < 0.05 and **p < 0.01 compared with AIA models; #p < 0.05 and ##p < 0.01 compared with QLY-treated AIA rats.

outcome was partially offset by NMN co-treatment (Figure 2B). In line with the results, Oil Red O staining-based histological examination discovers that QLY significantly restored fat decline in AIA rats' liver, but NMN reversed this trend (Figure 2C). Expression changes of SIRT1 and the related signals were much more significant in liver than those observed in blood (Figure 2D). SIRT1 as well as fat utilization-related proteins including HSL, ATGL and CPT-1A were all overexpressed in AIA rats' liver, while PGC-1α expression was reduced. These changes were possibly related to the inhibited status of PPARγ, whose expression and acetylation were both down-regulated.[36] QLY therapy led to significant restoration of these abnormalities, which should account for increased TG deposits. NMN antagonized the effects of QLY in this aspect once again (Figure 2E). The above findings show that SIRT1 signaling alteration was much more persistent and profound in metabolic organs than that in immune system.

QLY-Caused SIRT1 Inhibition Reshaped Status of AIA Rats' WAT

Fat deposits differences among these rats were significant (Figure 3A). QLY enlarged the shrunk WAT in AIA rats, while NMN exhibited an inhibitory effect against it (Figure 3B). AIA rats' adipocytes showed the reduced size. QLY exerted

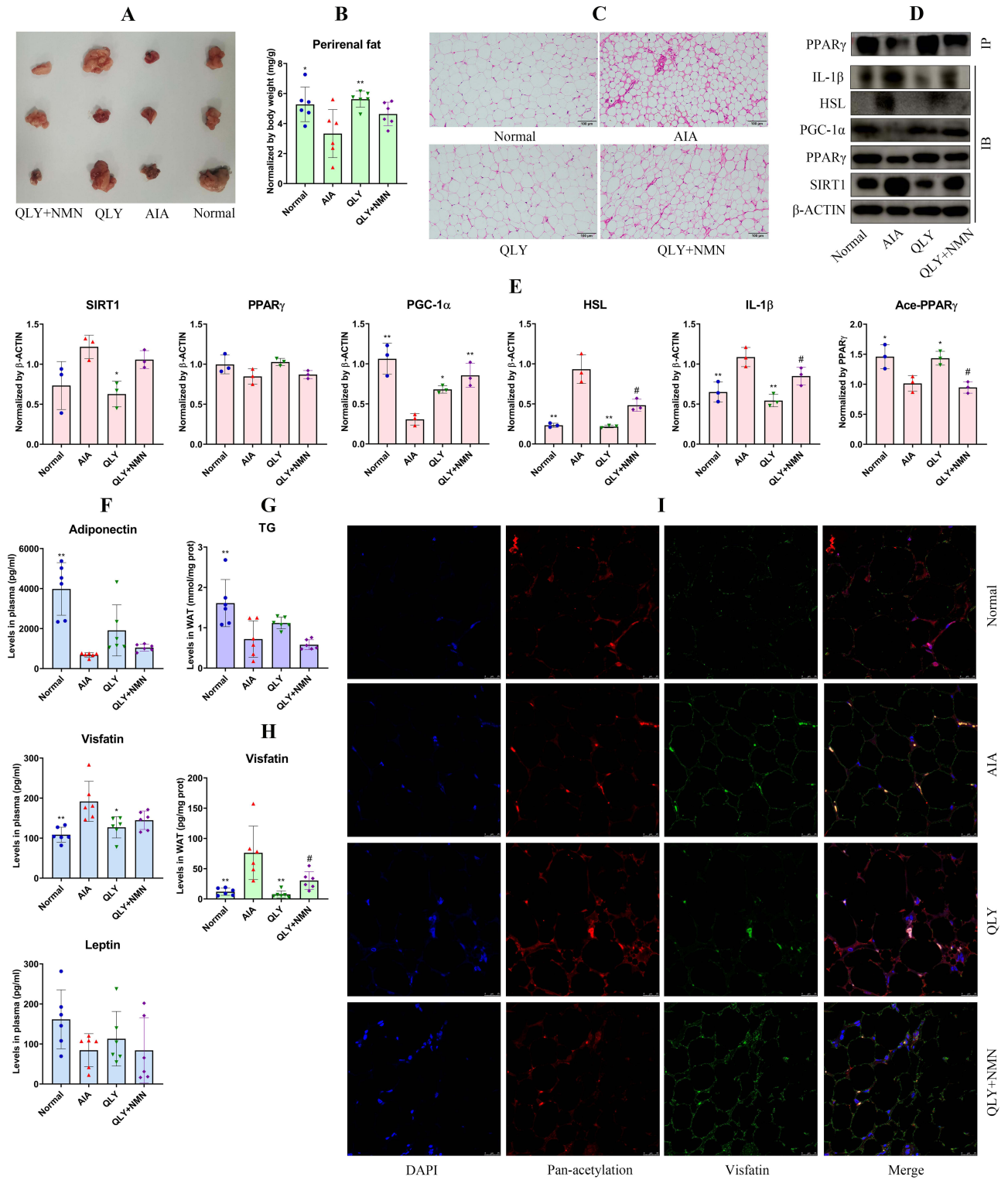

Figure 3 QLY therapy reshaped both metabolism and secretion of WAT in AIA rats by regulating SIRT1-related signals. (**A**) morphological observation of representative perirenal fat pads; (**B**) relative weight of perirenal fat pads; (**C**) H&E staining-based histological examination of perirenal fat pads; (**D**) WB and IP assays performed using rats' WAT samples; (**E**) the quantification results of assay (**D**); (**F**) levels of representative adipokines (leptin, adiponectin, and visfatin) in rats' blood; (**G** and **H**) TG and visfatin detected in rats' WAT; (**I**) expression of pan-acetylated proteins and visfatin in rats' WAT. All the data are presented in mean±SD. Statistical significance: *p < 0.05 and **p < 0.01 compared with AIA models; #p < 0.05 compared with QLY-treated AIA rats.

a restorative effect in this regard. NMN counteracted this result (Figure 3C). Besides metabolic regulators, we detected IL-1β and pan-acetylation (ace-lys) antibody-bound PPARγ in WAT to better interpret implications of SIRT1 changes there (Figure 3D). Expression differences of SIRT1, HSL and other metabolic regulators among these groups were very similar to those observed in liver. AIA-caused IL-1β increase was reduced by QLY, which was reversed by NMN. Meanwhile, PPARγ deacetylation was facilitated in AIA rats. QLY hampered the process. This function of QLY was thoroughly abrogated by NMN (Figure 3E). The facts solidly support that claim that QLY acted as a SIRT1 inhibitor in AIA rats' WAT. Because WAT is a potent secretion organ, we examined levels of adipokines in these rats' plasma. Adiponectin and leptin were significantly reduced in AIA rats, but visfatin levels were increased a lot. QLY reversed all these changes, and its effect on visfatin was especially efficient. NMN constrained QLY-brought effects to certain extends (Figure 3F). Then, we quantified some indicators in WAT to validate the above results. TG contents differences in these rats' WAT were consistent to the results of morphological/histological observations (Figure 3G). Visfatin levels variation there was similar to that observed in blood too, while the differences among groups were greatly amplified (Figure 3H). Meanwhile, AIA WAT expressed higher levels of visfatin than normal controls, and expression of pan-acetylated proteins in cytoplasm was reduced. After QLY treatment, acetylation was apparently promoted, and this phenomenon was coincided to visfatin decrease. These effects were abrogated by NMN (Figure 3I). The changes of (ace)-PPARγ and its downstream targets together with metabolic improvement in WAT confirm that QLY functionally inhibited SIRT1. This signal change affected adipokines network too, leading to obvious visfatin decrease.

QLY Exerted Indirect Anti-Inflammatory Effects by Regulating Pre-Adipocytes

In in vitro experiments, we first validated the impacts of different microenvironments on rat pre-adipocytes by WB method (Figure 4A). Compared with the result observed in vivo, AIA rats' serum caused even more dramatic increase of SIRT1 and HSL in the cells. Visfatin is an inflammatory adipokine derived from NAMPT. We therefore also investigated this protein, whose expression was up-regulated under this condition. QLY suppressed all the proteins' expression (Figure 4B). Comparatively, expression differences of PGC-1α and PPARγ among the groups were less obvious. Changes of SIRT1 and the related proteins led to the varied metabolic status. Levels of GLU and TG in the medium from QLY-treated AIA rats' serum-cultured cells were significantly up-regulated compared with AIA group, while LA was reduced (Figure 4C). It further indicates inhibitory effects of QLY on lipolysis and fat utilization. AIA serum induced IL-6, TNF-α and visfatin increase in pre-adipocytes. QLY-containing serum decreased their production. Visfatin was more sensitive to the environment than the other two (Figure 4D). Rat monocytes released more IL-1β, IL-6, and TNF-α, when stimulated with the medium from AIA serum-cultured rat pre-adipocytes. QLY-containing serum impaired its pro-inflammatory ability (Figure 4E). It is noteworthy that level changes of these cytokines were more significant than that observed in the in vivo experiment, confirming that WAT plays a pro-inflammatory role in AIA and drives pathological changes in certain tissues when immune alteration is spontaneously recovered. In line with this hypothesis, AIA rats' WAT homogenates increased IL-1β production in monocytes by nearly 3-folds, but the samples from QLY-treated AIA rats were unable to achieve this outcome (Figure 4F). The obtained clues suggest that QLY improved WAT-mediated inflammation by inhibiting SIRT/visfatin in AIA rats.

QLY Prevented Inflammatory Secretion of Pre-Adipocytes by Inhibiting SIRT1

We treated pre-adipocytes with QLY-containing serum and QLY-related compounds to confirm whether QLY indeed prevents them from acquiring inflammatory phenotype by inhibiting SIRT1. The selection of QLY-derived SIRT1 agonists and their treatment concentrations was in accordance with our previous studies.[24,25] We first investigated their impacts on SIRT1 and its rival PPARγ in the cells in the context of AIA serum stimulus (Figure 5A). Similar to QLY-containing serum, the compounds suppressed SIRT1 expression in AIA serum-primed pre-adipocytes, but increased expression of PPARγ and PGC-1α (Figure 5B). They showed the similar impacts on extracellular GLU and TG. However, QLY did not affect LA production this time (Figure 5C). The results were similar to those in the above experiments. It further confirms that SIRT1 inhibitors in QLY favor TG deposits. In the secretion aspect, both the compounds and QLY-containing serum had no impacts on adiponectin and leptin, but significantly inhibited AIA serum-induced visfatin production. Levels of inflammatory cytokines IL-1β, IL-6 and MCP-1 were all increased by AIA serum.

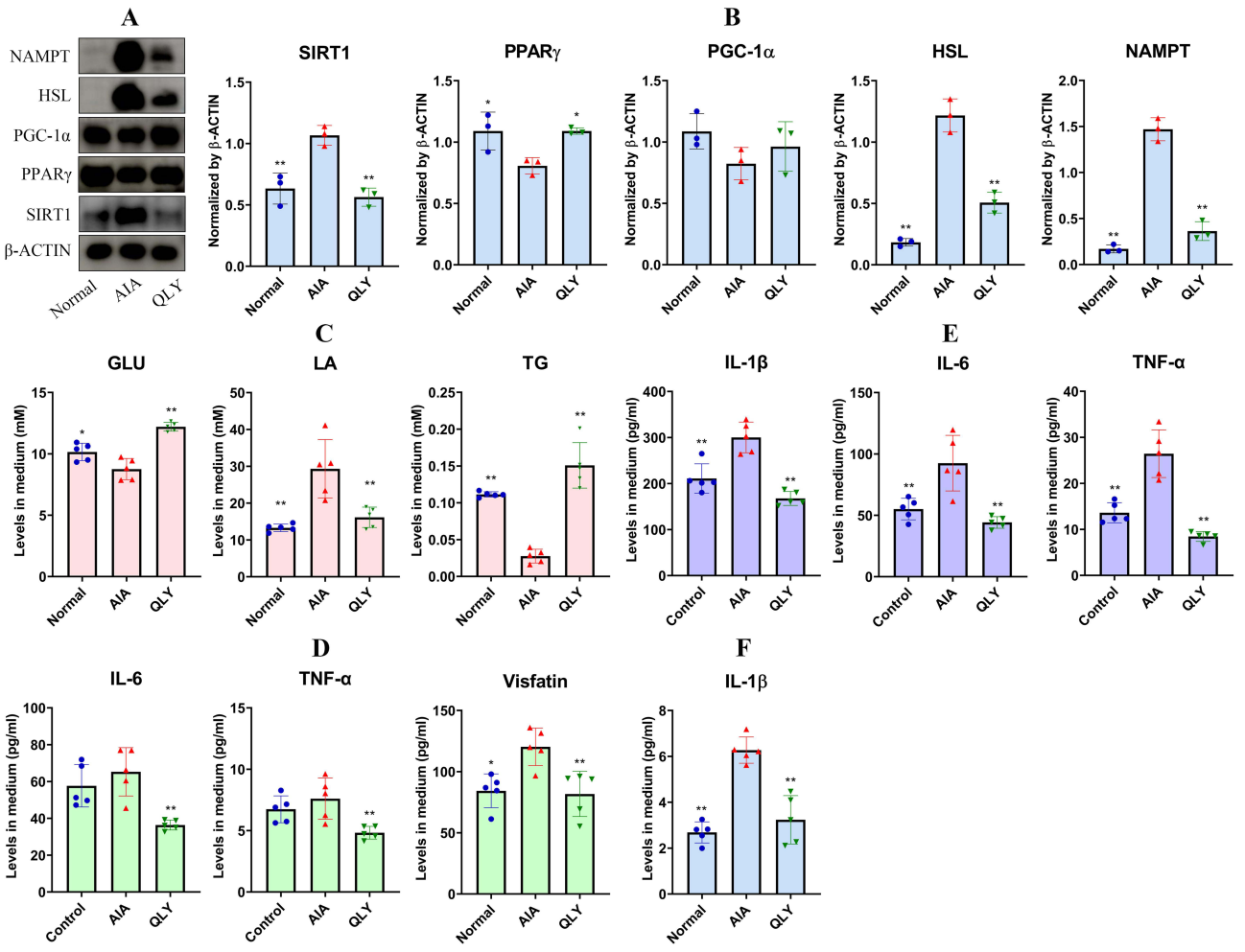

Figure 4 QLY-containing serum affected immune status of monocytes indirectly via pre-adipocytes. (**A**) WB assays performed using the rat pre-adipocytes, which were cultured with the serums from healthy, AIA model or QLY-treated AIA rats; (**B**) the quantification results of assay (**A**); (**C**) levels of some key metabolites (GLU, TG and LA) in the medium from assay (**A**); (**D**) levels of IL-6, TNF-α and visfatin in the medium from assay (**A**); (**E**) levels of IL-1β, IL-6, and TNF-α secreted by the monocytes cultured by the mediums from assay (**A**); (**F**) levels of IL-1β secreted by the monocytes cultured by the supernatants of different rats' WAT homogenates. All the data are presented in mean±SD. Statistical significance: *$p < 0.05$ and **$p < 0.01$ compared with AIA group.

QLY and the compounds generally brought their levels down. Comparatively, their effects on IL-1β were weak (Figure 5D). QLY-related treatments were especially effective in reducing visfatin, which was confirmed by a 3T3-L1 cells-based validation experiment (Figure 5E). IF assay further demonstrates that QLY-induced visfatin decline was related to increased acetylation (Figure 5F). Based on the collective data, we conclude that QLY and the related SIRT1 inhibitors do not suppress the overall secretion of WAT, but selectively controls visfatin release.

Then, we intended to confirm the beneficial consequences from SIRT1 inhibition. In WB assays, SIRT1 overexpression mimicked AIA rats' serum-caused changes in pre-adipocytes (Figure 6A). They both promoted expression of SIRT1 and NAMPT and decreased expression of PPARγ and PGC-1α. QLY-related compounds reversed these changes, and this outcome was partially offset by SIRT1 overexpression (Figure 6B). QLY-related compounds restored extracellular GLU and TG decline in AIA rats' serum-cultured cells. Although SIRT1 overexpression alone did not affect levels of the nutrients, it impaired metabolic regulation effects of the compounds. Interestingly, we observed that SIRT1 overexpression and the chemicals synergistically inhibited LA production (Figure 6C). These observations suggest that AIA condition had already sufficiently activated SIRT1; QLY-induced SIRT1 inhibition curbed fat utilization but did not contribute to glycolysis down-regulation. SIRT1 overexpression significantly reduced IL-6 expression, indicating an anti-inflammatory property of SIRT1. But it did not affect MCP-1 and visfatin, whose production would be either unaffected

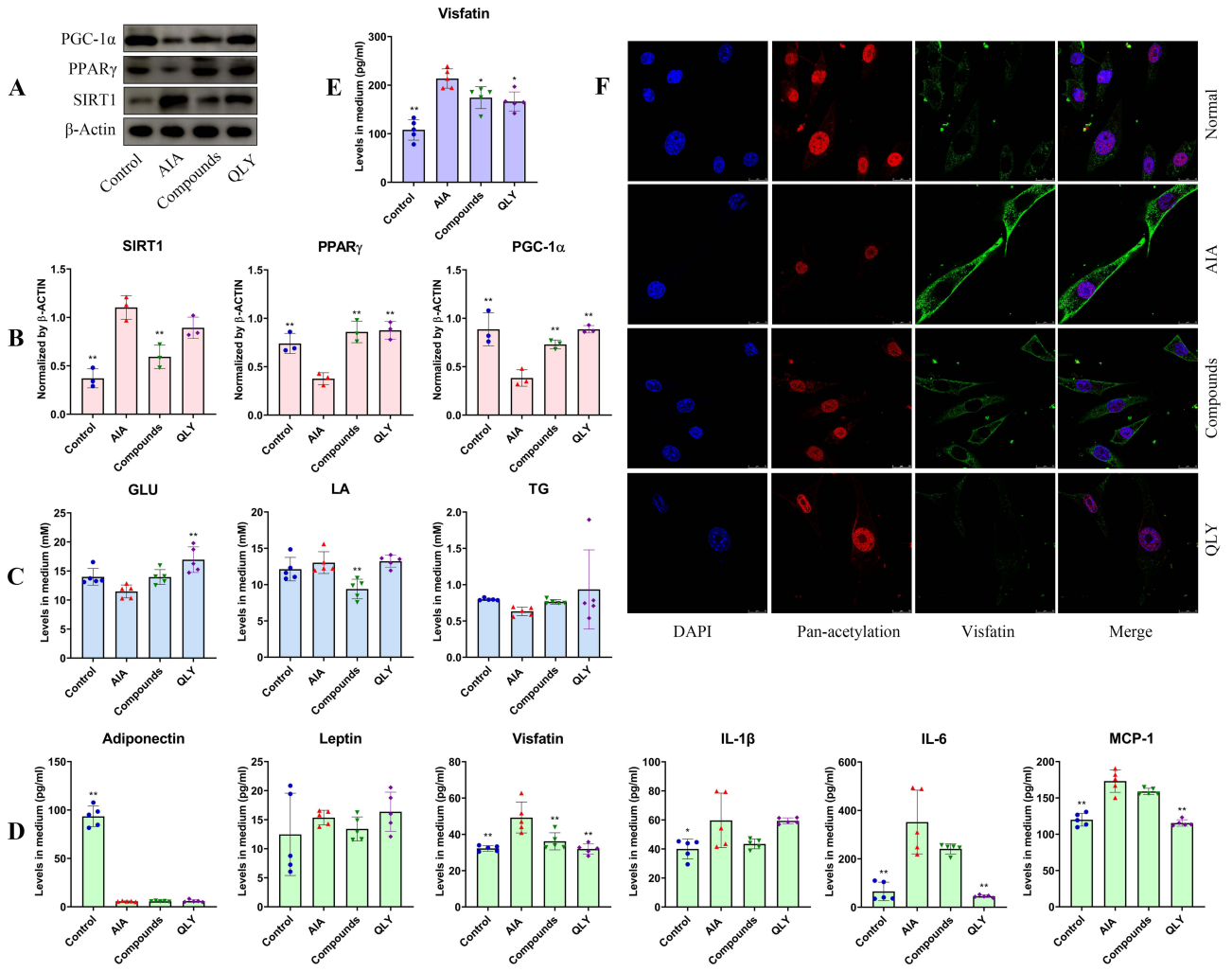

Figure 5 QLY-related SIRT1 inhibitors exerted the similar effects on pre-adipocytes to QLY-containing serum. (**A**) WB assays performed on the rat pre-adipocytes, which were cultured by healthy, AIA model rats' serums and then treated by the compounds or QLY-containing serum; (**B**) the quantification results of assay (**A**); (**C**) levels of some key metabolites (GLU, TG and LA) in the medium above; (**D**) levels of representative adipokines and cytokines (leptin, adiponectin, visfatin, IL-1β, IL-6 and MCP-1) in the medium; (**E**) levels of visfatin secreted by the 3T3-L1 cells, which received the same treatments as above; (**F**) expression of pan-acetylated proteins and visfatin in the cells from assay E. All the data are presented in mean±SD. Statistical significance: *p < 0.05 and **p < 0.01 compared with AIA group.

or promoted by SIRT1. QLY-related compounds reduced secretion of IL-6 and MCP-1, while this effect was antagonized by SIRT1 overexpression more or less (Figure 6D).

SIRT1-silencing in rat pre-adipocytes basically achieved an opposite outcome to SIRT1 overexpression in WB assays (Figure 6E). In fact, its effects were very similar to those induced by QLY-related compounds (Figure 6F). SIRT1-silencing reduced IL-6 production in AIA serum-cultured pre-adipocytes too, but it did not affect effects of the compounds in this aspect. It demonstrates the dual impacts of SIRT1 on IL-6. Similar to SIRT1 overexpression, its silencing exerted no effect on MCP-1 either. It confirms that SIRT1 does not control MCP-1 expression in WAT. SIRT1-silencing achieved a similar inhibitory effect on visfatin secretion to QLY-related compounds (Figure 6G). The collective data exhibit that visfatin decrease is a main benefit from QLY-induced SIRT1 inhibition in WAT, which would then prevent NF-κB activation in residential monocytes/macrophages.[21] Indeed, the abundant visfatin in the medium from AIA serum-cultured pre-adipocytes bound to THP-1 cells, and led to p65 subunit nuclear translocation. By decreasing visfatin, QLY-related SIRT1 inhibitors reduced p65 aggregation in nuclear (Figure 6H).

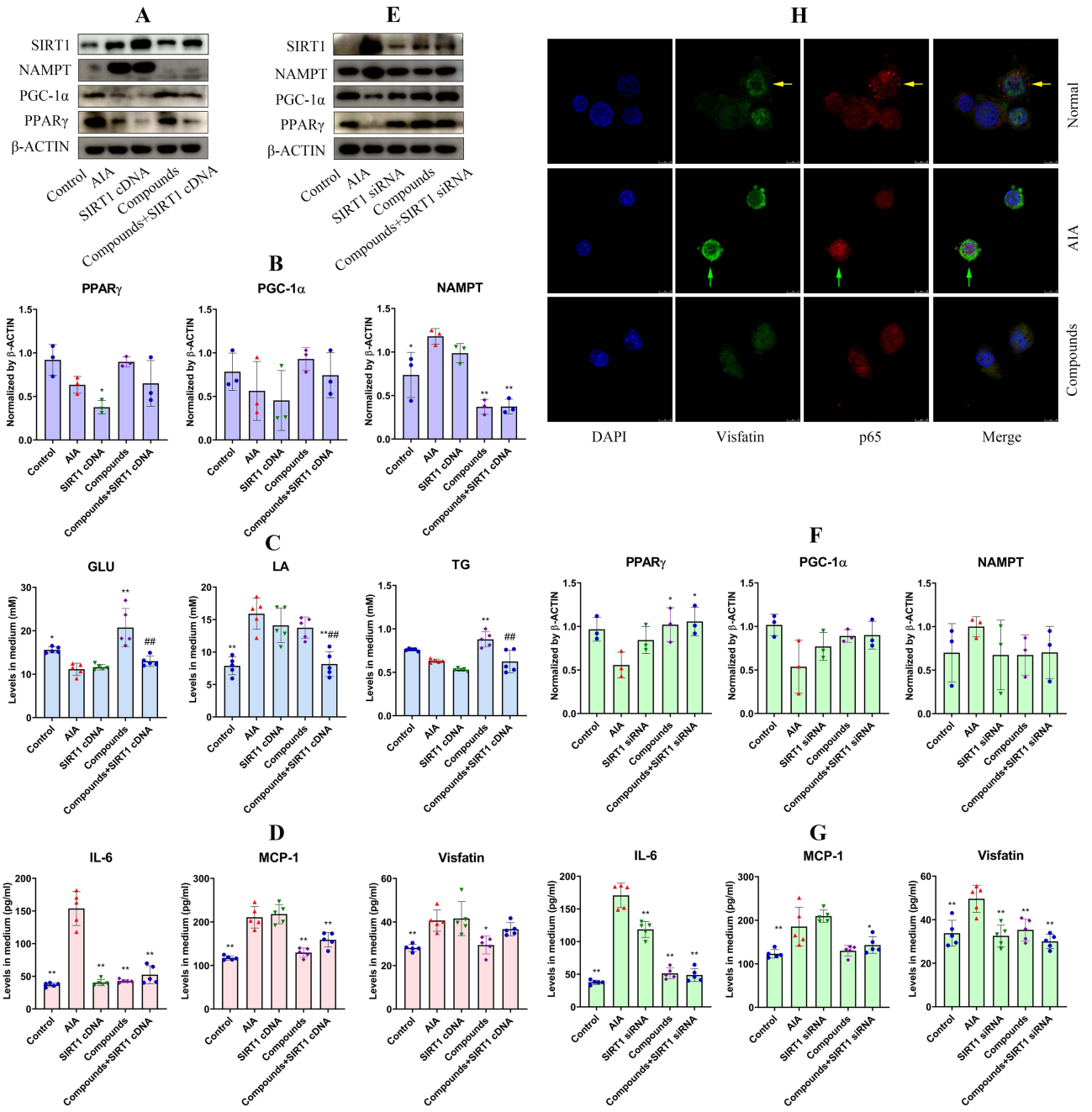

Figure 6 QLY-induced visfatin decrease in pre-adipocytes was attributed to SIRT1 inhibition. (**A**) WB assays performed using the pre-adipocytes cultured in vitro; SIRT1 in some of them were overexpressed, a portion of which were exposed to QLY-related SIRT1 inhibitors; (**B**) the quantification results of assay (**A**); (**C**) levels of some key metabolites (GLU, TG and LA) in the medium from assay (**A**); (**D**) levels of representative WAT-released substances (visfatin, IL-6 and MCP-1) in the medium; (**E**), WB assays performed using the pre-adipocytes cultured in vitro; SIRT1 in some of them were silenced, a portion of which exposed to QLY-related SIRT1 inhibitors; (**F**) the quantification results of assay (**E**); (**G**) levels of WAT-released substances in the medium from assay (**E**); (**H**) expression and localization of visfatin and p65 in the THP-1 cells stimulated by some mediums from assay (**A**); the yellow and green arrows indicate p65 distribution in the cytoplasm of normal cells and visfatin-induced p65 aggregation in the nuclear of AIA serum-cultured cells, respectively. All the data are presented in mean±SD. Statistical significance: *$p < 0.05$ and **$p < 0.01$ compared with AIA group; ##$p < 0.01$ compared with compounds group.

Discussion

RA is a very sophisticated condition with both immune and metabolism abnormalities. Being an inflammatory disease, great attentions are attached on the immune system. Indeed, many immune cells have been confirmed with involvement in RA pathology, including lymphocytes, monocytes/macrophages, granulocytes, and dendritic cells.[37] Biological agents are being developed based on this understanding. However, none of available immune regulation-based therapies can

thoroughly cure RA. Possibly, there exist some other players in RA. WAT is a good representative, which is not simply a fat deposit, but also actively participates in immune regulation via adipokines.

The observation lasted for 38 days here. By the end of experiment, normal and AIA groups showed similar levels of most immune indicators. *IL-6* expression was even decreased in AIA rats (Figure 1C–E). This result challenges the traditional view, as people tend to believe that RA is always accompanied with inflammation. But in fact, RA-related severe inflammation usually coincides to anti-inflammatory system up-regulation. It promises the spontaneous remission, and inflammatory cytokines are eventually declined during this stage.[8] This fact exhibits that RA is a self-limiting disease. We observed that joint injuries in AIA model rats were still vivid when they were killed (Figure 1F and H). Without immune hyper-activation, this condition allowed us to focus on WAT. As anticipated, metabolism and secretion changes there were notable (Figure 3), highlighting its possible role in RA pathology.

Besides immune system, WAT is another main source of inflammatory cytokines. We have recently confirmed that WAT is an effective amplifier of RA-related immune abnormalities, the functions of which are mediated by certain metabolic pathways.[38] The functional rivals SIRT1 and PPARγ are attracting research objects in this aspect because they regulate both fat metabolism and immune functions. We emphasized on PPARγ previously, due to its well-known anti-inflammatory nature.[23,24] A recent work discovers that QLY contains some compounds that effectively inhibit SIRT1 activity.[26] PPARγ activation may be partially attributed to this medicinal property. The current study validated this hypothesis. Expression changes of PPARγ and its downstream proteins as well as metabolic alteration in AIA rats' liver (Figure 2) and WAT (Figure 3) were all restored by QLY therapy. More importantly, ace-PPARγ expression decline was prevented, serving as a solid evidence for SIRT1 inhibition.

SIRT1 is a negative regulator of inflammation in monocytes/macrophages, but it promotes visfatin secretion in WAT.[16–20] The above change would cause complicated consequences. In previous studies, SIRT1 agonists notably restrained inflammatory polarization of monocytes and angiogenesis in AIA rats.[39,40] The results show that SIRT1 activation is generally beneficial when immune hyper-activation is significant. This work was performed during a remission stage of AIA to focus on the contribution of SIRT1 inhibition in WAT to the anti-rheumatic effects of QLY. QLY-caused SIRT1 inhibition reshaped secretion profile of WAT, but the conflicting data about adipokine changes were observed in the in vivo and in vitro experiments. The uncertainty should be attributed to varied immune environments.[38] Nonetheless, visfatin decrease under QLY treatment was reliable, making it a preferential research target in the following experiments. Our evidences confirm that its decline was related to SIRT1-mediated deacetylation (Figures 3I and 5F). It led to NF-κB down-regulation in the co-existing monocytes and reduced inflammation (Figure 6H). However, SIRT1 inhibition would also provoke inflammation because SIRT1 negatively controls transcriptional activities of NF-κB and AP-1.[16] It explains why QLY did not achieve therapeutic effects strictly in the dose-dependent manner and promoted inflammation conditionally.[25,26]

The above facts suggest that QLY therapy achieves indirect anti-inflammatory effects on monocytes/macrophages, and SIRT1 inhibition is meaningful in this aspect. Indeed, the direct effects of QLY-related compounds on monocytes are weak.[25] In fact, QLY-induced SIRT1 inhibition does not only contribute to this outcome via WAT but also affect T cells. QLY preferentially targeted T cells when treating AIA rats, whose changes prevented inflammatory polarization of monocytes/macrophages.[25] Of note, Th17 cells distribution was profoundly decreased. Interestingly, their differentiation is controlled by RORγt, a deacetylation target of SIRT1.[41] It is highly possible that QLY suppresses Th17 differentiation by inhibiting RORγt due to SIRT1 inhibition. As we know, synovial fibroblasts execute joint injuries in RA.[42] QLY can efficiently suppress their proliferation and the consequent synovial hyperplasia.[26] Synovioblasts with the elevated SIRT1 levels exhibit resistance to apoptosis and display particularly notable pathological activities.[18] The favorable effects of QLY on these cells are very possibly related to SIRT1 inhibition too. These clues imply that QLY-caused SIRT1 inhibition may benefit anti-rheumatic therapies in many aspects.

Conclusion

QLY therapy caused SIRT1 inhibition in AIA rats, leading to metabolic improvement in both liver and WAT. Meanwhile, this signal change reshaped secretion of WAT, and reduced visfatin production. It prevented the stimulus of visfatin on NF-κB and eased inflammation in co-existing monocytes/macrophages, which subsequently resulted in decreased

secretion of IL-6, MCP-1 and some other inflammatory cytokines. These results suggest that QLY anti-rheumatic therapy indirectly suppresses inflammation by inhibiting SIRT1 in WAT, and QLY has certain potentials in treating WAT-mediated diseases like obesity. Furthermore, it reminds us about possible unfavorable outcomes from the use of SIRT1 agonists as anti-inflammatory agents.

Abbreviation

NAD, nicotinamide adenine dinucleotide; RA, rheumatoid arthritis; WAT, white adipose tissues; TCM, Traditional Chinese Medicine; QLY, Qing-Luo-Yin; AIA, adjuvant-induced arthritis; BCG, Bacillus Calmette-Guérin; IFA, incomplete Freund's adjuvant; CFA, complete Freund's adjuvant; BSA, bovine serum albumin; FBS, fetal bovine serum; GSH, reduced glutathione; MDA, malonaldehyde; SOD, superoxide dismutase; AKP, alkaline phosphatase; GSP, glycated serum protein; GLU, glucose; LA, lactic acid; TG, triglyceride; T-CHO, total cholesterol; HDL-C, high-density lipoprotein cholesterol; LDL-C, low-density lipoprotein cholesterol; NMN, nicotinamide mononucleotide; WB, western-blot; IP, immunoprecipitation; qRT-PCR, quantitative reverse transcription polymerase-chain reaction; IF, immunofluorescence; RF, rheumatoid factor.

Data Sharing Statement

All data generated or analyzed during this study are included in this article and the Supplementary Information.

Ethics Approval

The animal study was approved by the Ethical Committee of Wannan Medical College (WNMC-AWE-2023358). The use of animals was adhered to the National Institutes of Health Guide for the Care and Use of Laboratory animals (2011), and all the experiment methods were in accordance with ARRIVE guidelines.

Funding

This work was supported by National Natural Science Foundation of China (82274465), Plans for Major Anhui Provincial Science & Technology Projects (202303a07020001), Excellent Research and Innovation Team of Anhui Provincial Colleges (2023AH010075), Scientific Research Project of Health Commission of Wuhu City (WHWJ2023y011), and Hengrui & Tianqing Medical Education Foundation (HXKT2022022).

Disclosure

The authors declare no conflict of interest.

References

1. McInnes IB, Schett G. The pathogenesis of rheumatoid arthritis. *N Engl J Med*. 2011;365(23):2205–2219. doi:10.1056/NEJMra1004965
2. Ding Q, Hu W, Wang R, et al. Signaling pathways in rheumatoid arthritis: implications for targeted therapy. *Signal Transduct Target Ther*. 2023;8(1):68.
3. Roberts CA, Dickinson AK, Taams LS. The interplay between monocytes/macrophages and $CD4^+$ T cell subsets in rheumatoid arthritis. *Front Immunol*. 2015;6:571. doi:10.3389/fimmu.2015.00571
4. Davignon JL, Hayder M, Baron M, et al. Targeting monocytes/macrophages in the treatment of rheumatoid arthritis. *Rheumatology*. 2013;52(4):590–598. doi:10.1093/rheumatology/kes304
5. Tu J, Huang W, Zhang W, Mei J, Zhu C. A tale of two immune cells in rheumatoid arthritis: the crosstalk between macrophages and T cells in the synovium. *Front Immunol*. 2021;12:655477. doi:10.3389/fimmu.2021.655477
6. Guo D, Lin C, Lu Y, et al. FABP4 secreted by M1-polarized macrophages promotes synovitis and angiogenesis to exacerbate rheumatoid arthritis. *Bone Res*. 2022;10(1):45. doi:10.1038/s41413-022-00211-2
7. Amoruso A, Sola D, Rossi L, et al. Relation among anti-rheumatic drug therapy, $CD14^+CD16^+$ blood monocytes and disease activity markers (DAS28 and US7 scores) in rheumatoid arthritis: a pilot study. *Pharmacol Res*. 2016;107:308–314. doi:10.1016/j.phrs.2016.03.034
8. Lei M, Tao M-Q, Y-J W, et al. Metabolic enzyme triosephosphate isomerase 1 and nicotinamide phosphoribosyltransferase, two independent inflammatory indicators in rheumatoid arthritis: evidences from collagen-induced arthritis and clinical samples. *Front Immunol*. 2021;12:795626. doi:10.3389/fimmu.2021.795626
9. Roszkowski L, Ciechomska M. Tuning monocytes and macrophages for personalized therapy and diagnostic challenge in rheumatoid arthritis. *Cells*. 2021;10(8):1860. doi:10.3390/cells10081860
10. Aletaha D. Precision medicine and management of rheumatoid arthritis. *J Autoimmun*. 2020;110:102405. doi:10.1016/j.jaut.2020.102405
11. Ali L, Schnitzler JG, Kroon J. Metabolism: the road to inflammation and atherosclerosis. *Curr Opin Lipidol*. 2018;29(6):474–480. doi:10.1097/MOL.0000000000000550

12. Qu W, Qiao S, Liu L, et al. Dectin3 protects against hepatocellular carcinoma by regulating glycolysis of macrophages. *Int Immunopharmacol*. 2022;113(Pt A):109384. doi:10.1016/j.intimp.2022.109384
13. Jones N, Blagih J, Zani F, et al. Fructose reprogrammes glutamine-dependent oxidative metabolism to support LPS-induced inflammation. *Nat Commun*. 2021;12(1):1209. doi:10.1038/s41467-021-21461-4
14. Yan J, Horng T. Lipid metabolism in regulation of macrophage functions. *Trends Cell Biol*. 2020;30(12):979–989. doi:10.1016/j.tcb.2020.09.006
15. Zheng Y, Wei K, Jiang P, et al. Macrophage polarization in rheumatoid arthritis: signaling pathways, metabolic reprogramming, and crosstalk with synovial fibroblasts. *Front Immunol*. 2024;15:1394108. doi:10.3389/fimmu.2024.1394108
16. Shen P, Deng X, Chen Z, et al. SIRT1: a potential therapeutic target in autoimmune diseases. *Front Immunol*. 2021;12:779177. doi:10.3389/fimmu.2021.779177
17. Wu YJ, Fang WJ, Pan S, et al. Regulation of Sirt1 on energy metabolism and immune response in rheumatoid arthritis. *Int Immunopharmacol*. 2021;101(Pt A):108175.
18. Niederer F, Ospelt C, Brentano F, et al. SIRT1 overexpression in the rheumatoid arthritis synovium contributes to proinflammatory cytokine production and apoptosis resistance. *Ann Rheum Dis*. 2011;70(10):1866–1873. doi:10.1136/ard.2010.148957
19. Cheng XP, Wang XW, Sun HF, et al. NAMPT/SIRT1 expression levels in white blood cells differentiate the different rheumatoid arthritis subsets: an inspiration from Traditional Chinese Medicine. *J Inflamm Res*. 2023;16:4271–4285. doi:10.2147/JIR.S431600
20. Yoon MJ, Yoshida M, Johnson S, et al. SIRT1-mediated eNAMPT secretion from adipose tissue regulates hypothalamic NAD^+ and function in mice. *Cell Metab*. 2015;21(5):706–717. doi:10.1016/j.cmet.2015.04.002
21. Garten A, Schuster S, Penke M, Gorski T, de Giorgis T, Kiess W. Physiological and pathophysiological roles of NAMPT and NAD metabolism. *Nat Rev Endocrinol*. 2015;11(9):535–546. doi:10.1038/nrendo.2015.117
22. Polyakova YV, Zavodovsky BV, Sivordova LE, Akhverdyan YR, Zborovskaya IA. Visfatin and rheumatoid arthritis: pathogenetic implications and clinical utility. *Curr Rheumatol Rev*. 2020;16(3):224–239. doi:10.2174/1573397115666190409112621
23. Zuo J, Wang X, Liu Y, et al. Integrating network pharmacology and metabolomics study on anti-rheumatic mechanisms and antagonistic effects against methotrexate-induced toxicity of Qing-Luo-Yin. *Front Pharmacol*. 2018;9:1472. doi:10.3389/fphar.2018.01472
24. Wang R, Li DF, Hu YF, et al. Qing-Luo-Yin alleviated monocytes/macrophages-mediated inflammation in rats with adjuvant-induced arthritis by disrupting their interaction with (pre)-adipocytes through PPAR-γ signaling. *Drug Des Dev Ther*. 2021;15:3105–3118. doi:10.2147/DDDT.S320599
25. Wang DD, Wu XY, Dong JY, et al. Qing-Luo-Yin alleviated experimental arthritis in rats by disrupting immune feedback between inflammatory T cells and monocytes: key evidences from its effects on immune cell phenotypes. *J Inflamm Res*. 2021;14:7467–7486. doi:10.2147/JIR.S346365
26. Ye P, Wang QH, Liu CS, et al. SIRT1 inhibitors within Qing-Luo-Yin alleviated white adipose tissues-mediated inflammation in antigen-induced arthritis mice. *Phytomedicine*. 2024;122:155132. doi:10.1016/j.phymed.2023.155132
27. Wang QH, Li Y, Dou DY, et al. Nicotinamide mononucleotide-elicited NAMPT signaling activation aggravated adjuvant-induced arthritis in rats by affecting peripheral immune cells differentiation. *Int Immunopharmacol*. 2021;98:107856. doi:10.1016/j.intimp.2021.107856
28. Liu JQ, Zhao XT, Qin FY, et al. Isoliquiritigenin mitigates oxidative damage after subarachnoid hemorrhage in vivo and in vitro by regulating Nrf2-dependent signaling pathway via targeting of SIRT1. *Phytomedicine*. 2022;105:154262. doi:10.1016/j.phymed.2022.154262
29. Zhang S, Zhu P, Yuan J, et al. Non-alcoholic fatty liver disease combined with rheumatoid arthritis exacerbates liver fibrosis by stimulating co-localization of PTRF and TLR4 in rats. *Front Pharmacol*. 2023;14:1149665. doi:10.3389/fphar.2023.1149665
30. Yin M, Ding X, Yin S, et al. Exosomes from hepatitis B virus-infected hepatocytes activate hepatic stellate cells and aggravate liver fibrosis through the miR-506-3p/Nur77 pathway. *J Biochem Mol Toxicol*. 2023;37(10):e23432. doi:10.1002/jbt.23432
31. Xu S, He L, Ding K, et al. Tanshinone IIA ameliorates streptozotocin-induced diabetic nephropathy, partly by attenuating PERK pathway-induced fibrosis. *Drug Des Devel Ther*. 2020;14:5773–5782. doi:10.2147/DDDT.S257734
32. Sun Y, Bai YP, Wang DG, et al. Protective effects of metformin on pancreatic β-cell ferroptosis in type 2 diabetes in vivo. *Biomed Pharmacother*. 2023;168:115835. doi:10.1016/j.biopha.2023.115835
33. Hua Z, Hui LI, Haihua W. Potential protective effects of the water-soluble Chinese propolis on experimental ulcerative colitis. *J Tradit Chin Med*. 2023;43(5):925–933. doi:10.19852/j.cnki.jtcm.20230727.002
34. Wang X, Shen C, Wang X, et al. Schisandrin protects against ulcerative colitis by inhibiting the SGK1/NLRP3 signaling pathway and reshaping gut microbiota in mice. *Chin Med*. 2023;18(1):112. doi:10.1186/s13020-023-00815-8
35. Recinella L, Orlando G, Ferrante C, Chiavaroli A, Brunetti L, Leone S. Adipokines: new potential therapeutic target for obesity and metabolic, rheumatic, and cardiovascular diseases. *Front Physiol*. 2020;11:578966. doi:10.3389/fphys.2020.578966
36. Harmon GS, Lam MT, Glass CK. PPARs and lipid ligands in inflammation and metabolism. *Chem Rev*. 2011;111(10):6321–6340. doi:10.1021/cr2001355
37. Aletaha D, Smolen JS. Diagnosis and management of rheumatoid arthritis: a review. *JAMA*. 2018;320(13):1360–1372. doi:10.1001/jama.2018.13103
38. Ye P, Wang QH, Kong WY, et al. White adipose tissue, a novel anti-rheumatic target: clues from its secretion capability and adipectomy-based therapy. *British J Pharmacol*. 2024;122:155132.
39. Wang DD, He CY, Wu YJ, et al. AMPK/SIRT1 deficiency drives adjuvant-induced arthritis in rats by promoting glycolysis-mediated monocytes inflammatory polarization. *J Inflamm Res*. 2022;15:4663–4675. doi:10.2147/JIR.S378090
40. Jiang TT, Ji CL, Yu LJ, et al. Resveratrol-induced SIRT1 activation inhibits glycolysis-fueled angiogenesis under rheumatoid arthritis conditions independent of HIF-1α. *Inflamm Res*. 2023;72(5):1021–1035. doi:10.1007/s00011-023-01728-w
41. Lim HW, Kang SG, Ryu JK, et al. SIRT1 deacetylates RORγt and enhances Th17 cell generation. *J Exp Med*. 2015;212(5):607–617. doi:10.1084/jem.20132378
42. Liu D, Kuang Y, Chen S, et al. NAT10 promotes synovial aggression by increasing the stability and translation of N4-acetylated PTX3 mRNA in rheumatoid arthritis. *Ann Rheum Dis*. 2024:ard–2023–225343.